SOLUTION MINING RESEARCH INSTITUTE

679 Plank Road
Clifton Park, NY 12065, USA

Telephone: +1 518-579-6587
www.solutionmining.org

Technical Conference Paper

1965 – 2025

Mechanical Integrity Tests in Salt Caverns: Modeling of the leakage of Nitrogen, Hydrogen and Methane through a given leak path to support tests interpretation

Vincent Barrere, Arnaud Réveillère, Mehdi Karimi Jafari

Geostock, France

SMRI Spring 2025 Technical Conference
27-29 April 2025
Wilhelmshaven, Germany

Solution Mining Research Institute Spring 2025 Conference

Wilhelmshaven, Germany, 27-29 April 2025

Mechanical Integrity Tests in Salt Caverns: Modeling of the leakage of Nitrogen, Hydrogen and Methane through a given leak path to support tests interpretation

Vincent Barrere, Arnaud Réveillère, Mehdi Karimi Jafari

Geostock SAS, 2 Rue des Martinets 92500 Rueil Malmaison, France

Abstract

Salt caverns have a unique property among large scale storages: their tightness can be accurately tested. This stems from the invention of the so-called Nitrogen / brine interface "Mechanical Integrity Test", developed in the US in the 1980s and that has since then imposed itself globally throughout the cavern storage industry, even if the practice and acceptance criteria still remains largely country and/or company-specific. To test the tightness of Hydrogen storage caverns, recent pilots HyStock (done in 2022), HyPSTER (2021-2024) and H2CAST (2022-2023) have all opted for first Nitrogen and then Hydrogen – brine interface tests while there is no technical obvious reason why a "standard" single Nitrogen test would not fit, as it does for a Methane cavern. It is likely due to the fact that MIT acceptance is largely experience-based which cannot be as strong for Hydrogen caverns, being only 6 caverns in a total of 2000 storage salt caverns. Available information from these pilots found no leak, whether it is with Nitrogen or Hydrogen. In order to assess the behavior in case of a leak, synthetic ones are assumed and modeled in this work. It aims to study the influence of the type of gas (Methane, Nitrogen and Hydrogen) on a leakage through the cementation of a casing by modeling the leak paths using three different approaches. The final objective is to compare leakage behavior with Methane, Hydrogen and Nitrogen, to support the standardization of testing protocols for Hydrogen caverns.

Key words: Mechanical Integrity Test, Hydrogen, Leak Path, Micro annulus, Salt Caverns

1. Introduction

1.1. Purpose of the work

Even though the feasibility of Hydrogen storage in salt caverns is not objected (6 caverns have been or are currently storing this gas), the renewed interest for this fluid as an energy carrier has prompted questions related to this new use at a much larger scale. Hydrogen storage in salt caverns is a gas storage, and is essentially similar to the most developed gas storage industry: natural gas storage. Started 65 years ago, circa. 700 natural gas caverns are in operation worldwide as of today. Hydrogen storage on salt caverns has to be built on the experience and standards it developed along the history of this industry.

One of these standards is the so-called Nitrogen / brine interface "Mechanical Integrity Test", developed in the USA in the 1980s and that have since then imposed itself globally throughout the cavern storage industry. The test procedure itself and the acceptance criteria may vary upon companies and/or countries, but are generally established. Successive projects in a given country/company use the same technique and acceptance criteria, in compliance with the relevant regulatory authority and company's standards. The procedures to execute a MIT for a Hydrogen storage cavern nevertheless do not have similar established guidelines.

In general, the MIT for natural gas caverns is conducted with an inert gas (Nitrogen) for practical reasons and to reduce impacts in case of a leakage. Given the difference in properties between Nitrogen and Hydrogen, questions remain on the recommended approach for Hydrogen storage caverns. Recently, several Hydrogen storage cavern pilots tackled it by conducting “combined MIT” consisting of a test with Nitrogen followed by a test with Hydrogen. When analyzing the HyStock and H2CAST tests both repeated with Nitrogen and Hydrogen, Buzogany et al. (2023) concluded that “No significant differences could be identified with regard to leak rates. Therefore, the presented results can be seen as initial field evidence that the Nitrogen MIT is also representative for Hydrogen storage as it is for other gas storage.”

Most importantly, it should be pointed out that in all these tests, whether it was with Nitrogen or Hydrogen, no leak was detected. These recent pilot projects that repeated MITs with Nitrogen and then Hydrogen are field observations, at scale, showing that when no leak is observed with Nitrogen, no leak is observed with Hydrogen. This result is a significant milestone. But unfortunately, since there is no leak, it does not help comparing what would be a leak rate with Hydrogen, Nitrogen or Methane, and as a consequence on whether we should change the way tests are done for Hydrogen caverns. In addition, in the case of caverns conversions, it still remains unclear whether the conclusions of Nitrogen MITs can be reused for future Hydrogen use.

To complement the in-situ Pilot approach that found no leak, this article considers several scenarios of hypothetical leak paths and computes actual leak rate for Nitrogen (N_2), Hydrogen (H_2) and Methane (CH_4) in order to compare them.

1.2. MIT principle

Since the decisive invention of the Nitrogen/brine Mechanical Integrity Tests (MIT) in the 1980’s (van Fossan, 1983), salt caverns have the singular advantage that their tightness can be tested very accurately. In its most standard field and interpretation practice today, it implies pressurizing the cavern with brine, injecting Nitrogen down to just below the last cemented casing shoe and running a log at the start and at the end of the test. Logs enable the measurement of the Nitrogen/brine interface depth (and hence deduce the volume of Nitrogen in the well) and a temperature log (and hence deduce a density log). From the volume and density of Nitrogen measured at the start and at the end of the test, a mass balance of the Nitrogen can be made, and leaks identified, if any. The very small volume, when compared to cavern’s one, enables the test to reach extremely good accuracy.

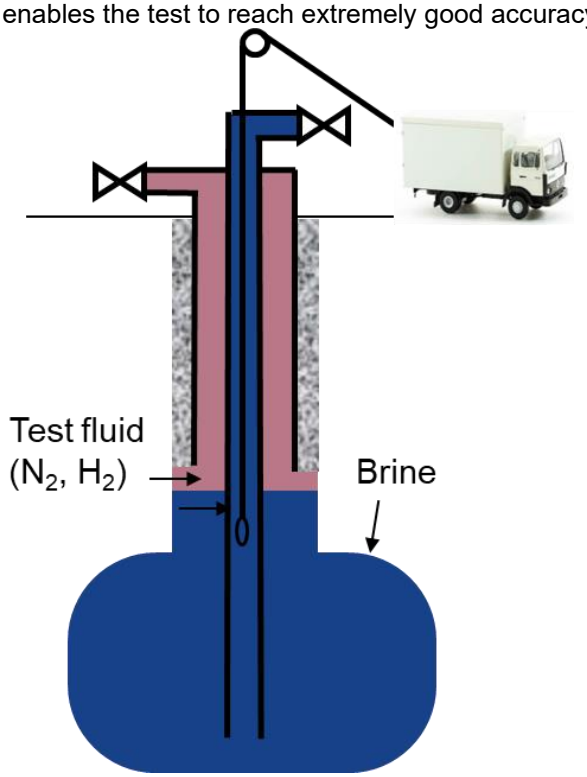

Figure 1: Schematic of The In-Situ Set-Up During a Nitrogen/Brine or Hydrogen/Brine MIT

Details on the development of accurate tightness test techniques in the salt cavern industries and of the concept of the MIT can be found in Réveillère, 2021. This work notably shows that the question of the acceptance criteria of MITs came along with the development of the tests. The first attempts were to relate a fail/pass criterion to the impact on groundwater (concept of Maximum Acceptable Leak Rate, MALR). It did not prove to be practical, as the occurrence of leak paths below ground is practically unpredictable and would be case-specific, which prevents it from setting an industry standard. The alternative approach was to base the test acceptance on the fact that a possible leakage cannot be distinguished from the accuracy of the test (concept of Minimum Detectable Leak Rate, MDLR) while setting stringent but achievable limits to the MDLR that must be met on the field. It is what is practiced today: MIT developers probably still have in mind what is desirable from a groundwater protection point of view, but also the practical impossibility to establish a quantitative MALR. And they can refer to the track record of several decades of salt cavern testing with an accuracy (MDLR) below the reference MDLR values of equivalent 1,000 bbl/y (in North America) or 50 kg/d (a figure proposed as a reasonable standard in Crotogino, 1995, probably the first significant attempt to standardize the MIT practice) or 50 l/d (in Europe), and to the limited history of leakage incidents from the salt cavern storage industry, especially when recent caverns are concerned. These threshold figures can be seen as typical accuracies that are commonly reached, for Nitrogen MITs.

1.3. Hydrogen, Methane and Nitrogen Properties

Hydrogen (H_2), Methane (CH_4) and Nitrogen (N_2) are three gases presenting different physical properties that can influence their flow. The differences between those three gases are illustrated by figure 2

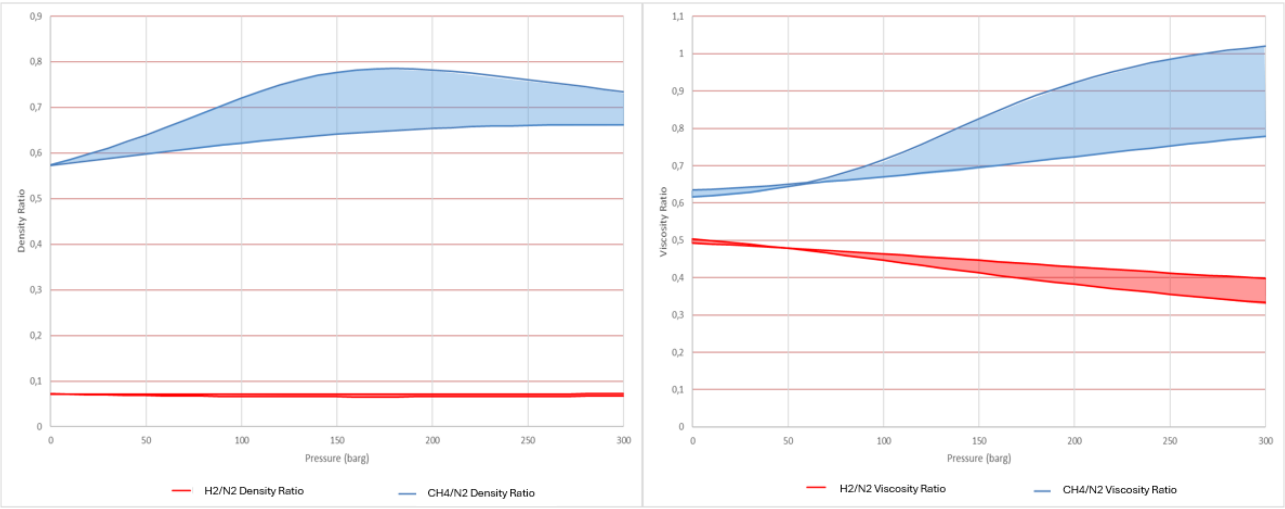

Figure 2: Comparison of the two envelopes of density and viscosity ratios Hydrogen/Nitrogen and Methane/Nitrogen considering a [0;100°C] Temperature range - (REFPROP Results)

From those graphs, it can be noted that Hydrogen is is a much lighter (14 to 15 times less dense) and less viscous (50 to 70% lower) gas than Nitrogen for the typical range of pressure ([0;300barg]) and temperature ([0;100°C]) generally considered for storage in underground salt caverns.

On the other hand, Methane and Nitrogen present more similar properties, even though Methane is 20 to 40% less dense and up to 40% less viscous than Nitrogen.

From those results, it can be intuited that the flow of Nitrogen and Methane through a given leak path may present a similar behaviour, on the contrary to Hydrogen that presents a higher mobility.

2. Modeling Approaches of a leak path through the cementation

2.1. Leak scenario: focus on a leak path through the cementation

In order to validate the first observations based on the different properties of these three gases and to quantify the impact of those properties on the resulting leak rate, it is important to understand the mechanisms in place through which the gas can leak out of the storage.

As previously stated, the salt formation being intrinsically tight (typical permeability is generally of 10^{-19} m^2), the testing of a well / underground storage often consists of assessing the tightness of its weakest mechanical point, which is the last cemented casing shoe: if the pressure builds up in a well, exceeding the maximum acceptable pressure, the first point at which leakage is really likely to happen is at this depth (Figure 3). The preferential leak path would then be driven by the direction of lower mechanical resistance, which generally goes vertically, through the cement sheath, either up to surface (pressure / leak visible in surface in the cemented annulus), or to a porous zone of lower pressure (e.g. Surface aquifers).

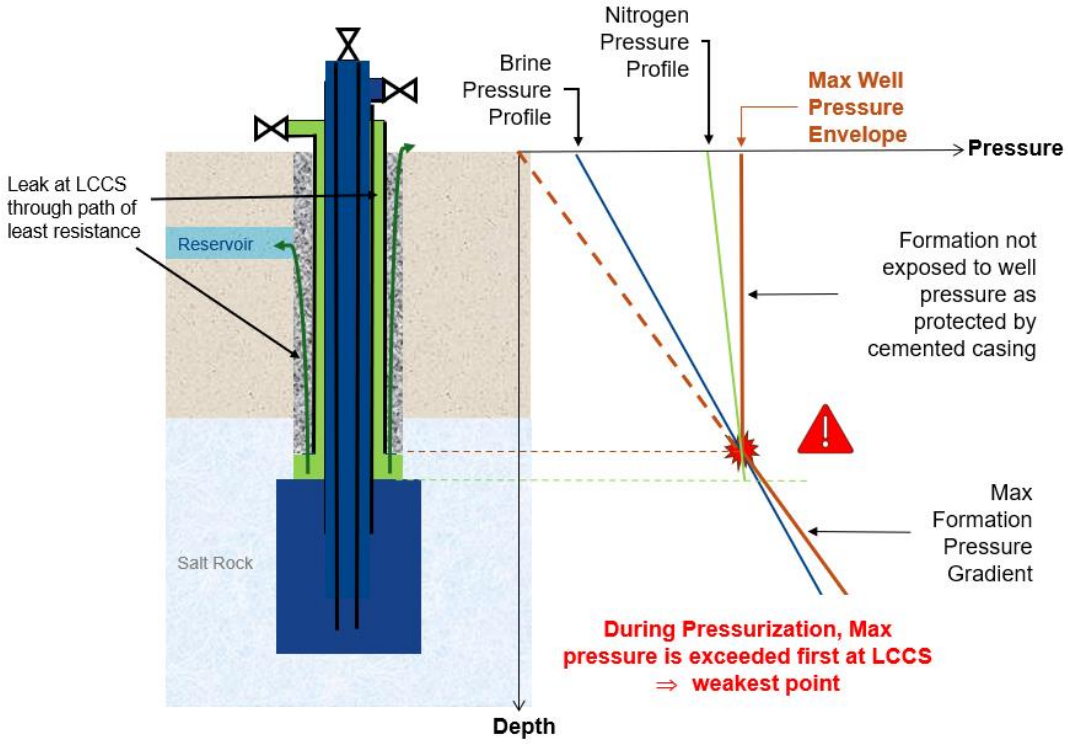

Figure 3: Schematic showing the main leak paths through the well during a test

Throughout its lifecycle, the well is submitted to various thermal and mechanical loadings that can change stresses through the cement, induce small cracks, connect existing defaults in the cementation (channeling, debonding of the cement from the casing and/or formation) and ease the migration of stored product through the cement.

This phenomenon is more critical at high pressure in the storage, and the highest pressure a cavern can see is applied during its mechanical integrity tests. The exact determination of the leak path geometry with regard to the geomechanical characteristics of the cementation as well as the flow regimes applicable for the fluid leaking through this latter nevertheless remains a difficult point to tackle.

The size and geometry of the leak path are highly case dependent (history of the well, success of the cementation, architecture of the well, local geology…), and therefore considering a unique geometry may be misleading. Similarly, the discussion regarding the flow regimes to apply in such complex structures may not be so straightforward, nor the interactions to consider between the fluid's properties in the leak path and the medium itself.

The general modeling of such site-specific phenomena turns out to be very complex as such, hence the decision to partition the problem into several simpler models that will be individually analyzed and compared in a second time. The next paragraphs aim to present three different approaches considered to model the leak paths through the cement sheath during a Mechanical Integrity Tests

- Fluid flow governed by the Darcy's law (flow through a porous medium in the cement, or through a hypothetical open micro annulus)
- Micro annular flow at the interface between the cement and the casing (flow through an annulus of small size with an elastic response depending on the internal and external stresses applied)
- Fluid flow through a channel (inside a circular tube or a uniform annular space between two concentric tubes) of a given size in the cement sheath

2.2. Model 1 – Micro annulus with a flow following Darcy's law (Poiseuille)

In this first hypothetical leakage scenario, the migration occurs through a micro annulus, typically at the formation/cement or cement/casing bonds, rather than through the cement matrix itself. This micro annulus is here assumed to be constantly open, of fixed size along the whole wellbore, and does not consider the dynamic behaviour of micro annuli (cf. next section).

From a flow modelling perspective, the micro annuli can be described in terms of their aperture, similar to how rock fractures are characterized (Stormont et al., 2018). The hydraulic aperture (e) is the spacing between smooth-walled parallel plates that produces the equivalent steady-state flow as the micro annulus. The hydraulic aperture of a micro annulus that corresponds to the effective permeability (k_{eff}) of a wellbore system can be approximated by the so-called cubic law:

$$k_{eff} \cdot A_{eff} = \frac{e^3 \cdot w}{12} \qquad (1)$$

Where A_{eff} is the wellbore annular effective area and w is the length of the hydraulic aperture, that can be approximated to the circumference of the casing assuming the micro annulus is at the casing/cement bond.

For this model, a micro annulus propagating from the cavern to surface was considered and potential capillary forces (caused by initial water in place) were neglected. The vertical Darcy single phase volumetric flow rate at a depth z is:

$$Q_L(z) = \frac{k_{eff} \cdot A_{eff}}{\mu(T,P)}\left(\frac{dP}{dz} - \rho(T,P) \cdot g\right) \qquad (2)$$

Since the leaking gas migrates upwards over several hundreds of meters, its density ρ and viscosity μ vary with respect to temperature and pressure.

The simulation of the flow rate is done by applying Darcy law in a porous column with decreasing density of the gas as it moves toward lower pressure zones.

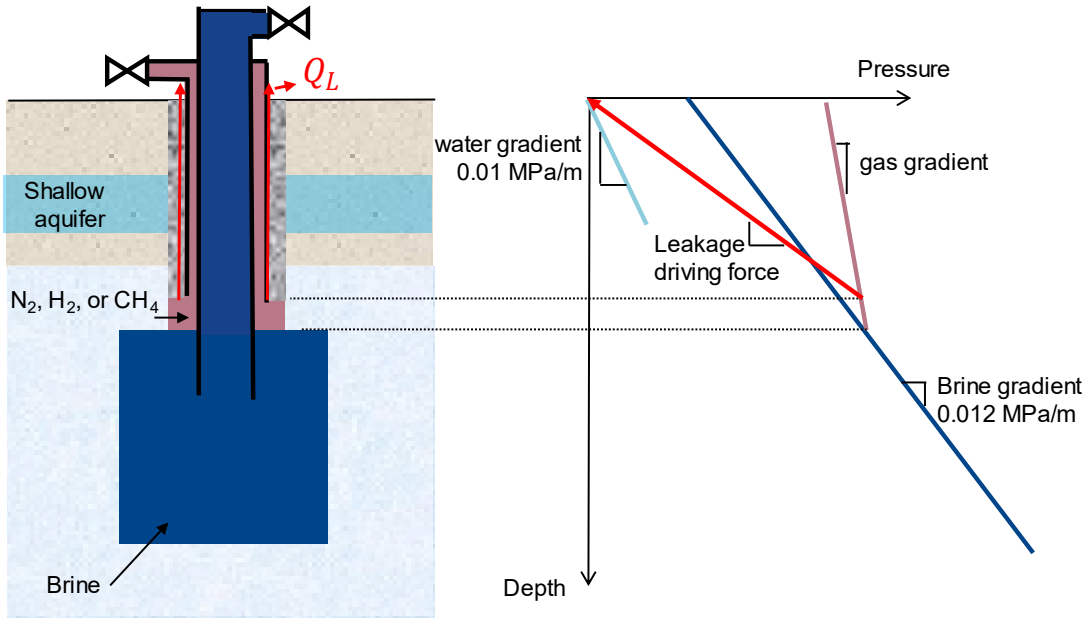

Figure 4: pressure profiles in the cavern and surrounding groundwater, and MIT test pressure gradient (in green). The micro annulus leak path is represented in red on the left schematic, and the driving force of it by the red arrow on the right diagram.

2.3. Model 2 – Micro annulus with elastic response

The previous model is therefore considering a flow through a path of small size that can be considered as a porous medium or a network of small fractures of a fixed size. The conceptualization of a micro annulus of a fixed geometry is nevertheless rather simple and may be misleading: in reality, the micro annulus is not a rigid object but presents an elastic behaviour. Its shape is thus impacted by the evolution of the internal pressure caused by the migration of gas through the leak path as well as the external stresses applied on this one (internal pressure in the well, overburden of the overlying formations…): a micro annulus will therefore tend to open and close through time, which results in an evolutive system with a varying size of the micro annulus and resulting flow rate, depending on local conditions.

The phenomenon is illustrated by Figure 5: under a certain pressure, the micro annulus can open and allow the gas to migrate through it. Frictions will cause a reduction of pressure along the path, which will cause a reduction of the micro annulus size, until the inner pressure is not sufficient to counteract the effect of external stresses, and lead to the closure of the path at a certain depth. The accumulation of gas at this depth will eventually increase the pressure locally, which will allow the reopening of the micro annulus and the upward migration of the trapped gas.

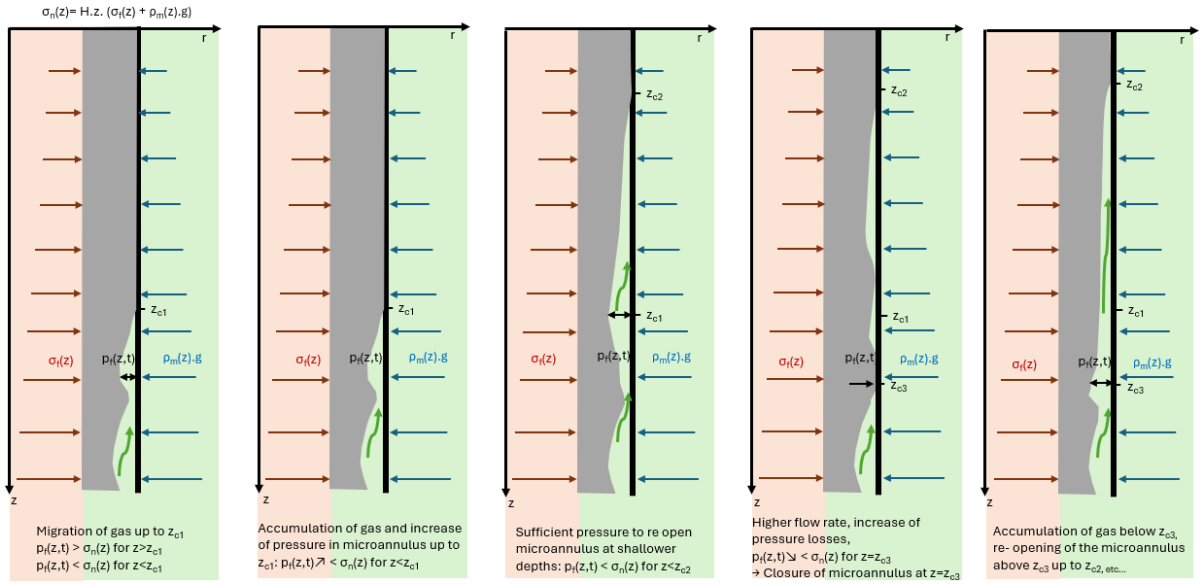

Figure 5: Illustration of the "geyser-type" flow for the micro annulus

Lecampion et al. presented in 2013 a mathematical solution to model such "geyser-type" flow. They introduced two key parameters that are the equivalent elastic modulus M of the micro annulus and the H factor accounting for the stress transfer between the inner and outer radius of the casing in the case of a fully bonded system casing/cement/formation.

The aperture $w(\theta)$ of the micro annulus is linked to the net inner pressure p by the following formula:

$$w(\theta) = 2\vartheta R\mathcal{F}(\theta,\vartheta)\frac{p}{M}, with\ \theta \in [-\vartheta, +\vartheta] \qquad (3)$$

Where

- $\theta \in [-\vartheta, +\vartheta]$ and ϑ the mid angle of the micro annulus (see figure 6)
- $2\vartheta R\mathcal{F}(\theta,\vartheta)$ a dimensionless function corresponding to the crack arc-length.
- p the net pressure: it is the difference between the inner pressure of fluid in the micro annulus ($p_f(z,t)$) and the external stresses applied on this one ($\sigma_n(z)$):

$$p = p_f(z,t) - \sigma_n(z) \qquad (4)$$

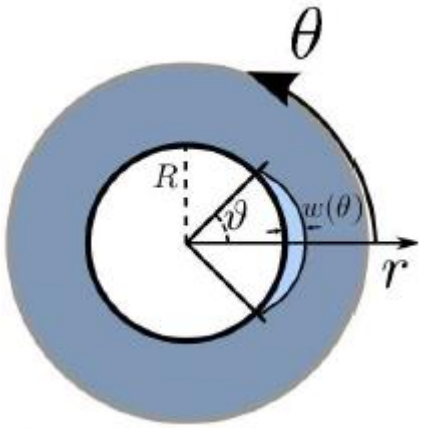

Figure 6: Illustration of the micro annulus geometry – horizontal cross section of the well (issued from Lecampion et al., 2013)

This second term is influenced by the pressure inside the casing (to simplify the fluid static pressure) and the pressure applied by the overlying formations: in the case of an ideal creeping formation pressure gradients up to 0.23bar/m can be considered to apply on the cement sheath, which is highly favorable to prevent leaks occurrences. This is nevertheless not always the case, and lower stresses can be considered.

The resulting stress transfer on the micro annulus can then be expressed by the introduction of the H parameter

$$p = p_f(z,t) - H.\left(p_{inner\ casing} + p_{external\ formation}\right) \quad (5)$$

By combining the two previous equations (4) and (5) to the continuity equation (6), and the expression of the flow rate derived from the fluid velocity profile given by Poiseuille's law (7), it is then possible to reach a system of four equations that can be solved numerically to evaluate the evolution of the flow rate, pressure, micro annulus aperture, fluid viscosity and fluid density

$$\frac{\partial A_c}{\partial t} + \frac{\partial Q}{\partial z} = 0 \quad (6)$$

$$Q(z) = -\frac{2R\vartheta\mathcal{C}}{12\mu_f} {w_o}^3 \left(\frac{\partial p_f}{\partial z} + \rho_f g\right) \quad (7)$$

Where

- $A_c(z,t)$ is the cross section of the crack and can be expressed as a function of $w_o(z,t)$:
  - $A_c = 2R\vartheta\mathcal{H}w_o$, with $2R\vartheta\mathcal{H}$ a function linked to the geometry of the crack
- $Q(z,t)$ is the volumetric flow rate through the leak path
- R the radius of the well,
- ϑ the mid angle of the crack,
- $\mathcal{C}$ a function linked to the geometry of the crack
- $w_o(z,t)$ the maximum aperture of the micro annulus.
- $\mu_f(z,t)$ the viscosity of the fluid in the micro annulus
- $\rho_f(z,t)$ the fluid density in the micro annulus
- g the gravitational constant on Earth: 9.81m.s^{-2}

This model is representative of most of the leak paths occurrences through the wells cement sheaths. Nevertheless, the numerous parameters required can make it harder to model than the two other models presented in this article. A certain number of assumptions have thus been made to simplify the resolution of this system and quickly evaluate the characteristics of the leak rate for the different fluids considered.

- Steady state flow: no dependence of the phenomenon to time, the mass flow rate is a constant
- Debonding at the interface between the casing and the cement ($\vartheta = \pi$)
- A plane-strain approximation (crack for which the axial length is much greater than the borehole radius and for a uniform net loading) applied to the case of a complete azimuthal debonding: in that case, it is possible to calculate the M and H factors with the Lamé solution (see equations (8) and (9)). The functions $\mathcal{F}$ and $\mathcal{C}$ are also simplified with this assumption: $\mathcal{F}(\vartheta = \pi) = \frac{1}{2\pi}$ and $\mathcal{C} = 1$

$$\frac{1}{M} = \frac{2{R_1}^2 + {R_2}^2(\chi_1 - 1)}{4\mu_1({R_2}^2 - {R_1}^2)} + \frac{{R_2}^2(\mu_2 - \mu_3)(\chi_2 - 1) + {R_3}^2(2\mu_2 + \mu_3(\chi_2 - 1)}{2\mu_2(2{R_2}^2(\mu_3 - \mu_2) + {R_3}^2(2\mu_2 + \mu_3(\chi_2 - 1))} \quad (8)$$

$$H = \frac{\mu_2(\chi_1 + 1)(2(\mu_3 - \mu_2) + {\alpha'}_2(R_3/R_1)^2)}{2\left((\mu_3 - \mu_2)\alpha_2 + (R_3/R_2)^2(\mu_2 - \mu_1){\alpha'}_2\right) + \alpha_1{\alpha'}_2(R_3/R_1)^2 + 2\kappa(R_2/R_1)^2(\mu_2 - \mu_3)} \quad (9)$$

Where

- The indexes 1, 2, 3 correspond respectively to the characteristics of the different materials: i=1 for casing steel, 2 for cement and 3 for formation- salt rock (see figure 7)
- $\mu_i = E_i/2(1+\nu_i)$
- $\chi_i = 3 - 4\nu_i$
- E_i is the Young modulus of the material i (i=1 for casing steel, 2 for cement and 3 for formation- salt rock)
- ν_i is the Poisson's ratio of the material i (i=1 for casing steel, 2 for cement and 3 for formation- salt rock)
- $R_i$is the radius of the corresponding material i (i=1 for casing steel, 2 for cement and 3 for formation-salt rock)
- $\alpha_1 = 2\mu_1 + \mu_2(\chi_1 - 1)$
- $\alpha_2 = 2\mu_2 + \mu_1(\chi_2 - 1)$
- $\kappa = \mu_1(\chi_2 - 1) - \mu_2(\chi_1 - 1)$
- $\alpha'_2 = 2\mu_2 + \mu_3(\chi_2 - 1)$

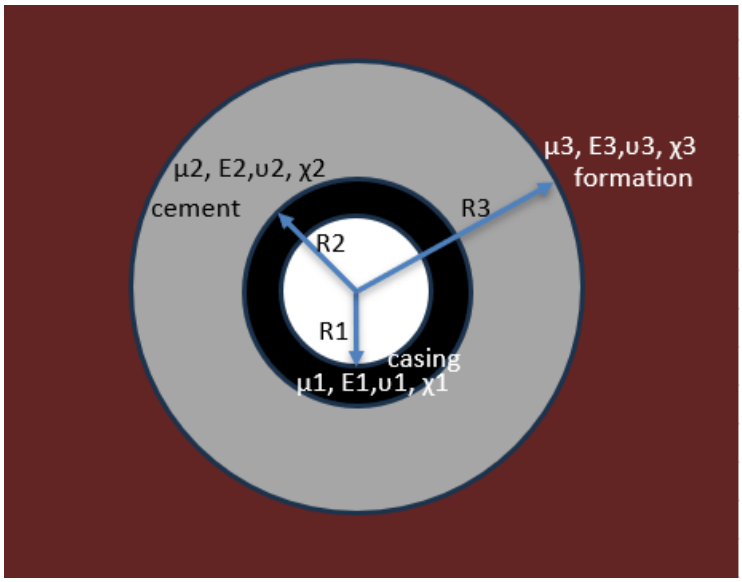

Figure 7: Illustration of the different parameters used in the Lamé solution for the calculation of H and M parameters

2.4. Models 3 and 4 - Channels with a pipe flow law

In this third model, the leak path is considered as a circular pipe or an annular space of constant section from the casing shoe level to the ground surface inside the cement sheath. The gas leakage is therefore modelled with a pipe flow law. This model consists of solving the system composed of the following equations:

- Real gas equation of state
- Mass balance
- Energy balance
- Momentum balance

The real gas equation is based on the gas compressibility factor that is calculated using REFPROP Algorithms as well as all other gas properties used in this system of equations.

Referring to SMRI report (Brouard consulting and RESPEC, 2013), the above cited equations allow to solve the pipe flow problem for a real gas as follows:

$$P = Z(P,T)\rho rT \tag{10}$$

$$u = \frac{\dot{m}}{\rho S} \tag{11}$$

$$\frac{\partial P}{\partial z} - \rho u^2 \left[\left(\frac{1}{P} - \frac{Z'_P}{Z}\right)P'_Z - \left(\frac{1}{T} - \frac{Z'_T}{Z}\right)T'_Z\right] + \rho g + sgn(u)\zeta(u,T) = 0 \tag{12}$$

$$C_P(T)\frac{\partial T}{\partial z} - \left[\frac{rT^2 Z'_T}{P}\right]\frac{\partial P}{\partial z} - u^2\left[\left(\frac{1}{P} - \frac{Z'_P}{Z}\right)P'_Z - \left(\frac{1}{T} - \frac{Z'_T}{Z}\right)T'_Z\right] + g = 0 \tag{13}$$

Where

- P, gas pressure
- T, gas temperature
- r=R/M, the ratio of gas constant over gas molar mass
- Z, compressibility factor of gas
- ρ, gas density
- m, mass of gas
- u, gas velocity in the pipe
- S, pipe cross section
- z, depth
- Cp, heat capacity of gas at constant pressure

In the momentum equation, ζ (u, T) represents the pressure loss:

$$\zeta(u,T) = \frac{f(u,T)}{2D}\rho u^2 \tag{14}$$

Where

- f, friction factor which is calculated as a function of Reynolds number
- D, pipe hydraulic diameter.

This system includes the energy balance equation for an adiabatic flow assumption. The present work nevertheless assumes that the gas has enough time to reach the thermal equilibrium with the rock mass: instead of solving the energy equation, the gas temperature is set to the rock mass temperature at each depth.

To solve the above system of equations, the following boundary conditions are set as follows:

- Pressure and temperature at casing shoe are set to downhole values.
- Temperature along the leak path is set to the rock temperature (thermal equilibrium assumption). In this case the energy balance equation is not used.
- Pressure at surface is set to atmospheric pressure if gas velocity is lower than the sound velocity at surface conditions (normal flow).
- When the gas velocity reaches sound velocity at surface, instead of atmospheric pressure, the gas velocity is set to the sound velocity as the boundary condition at surface (chocked flow).

This flow model will be applied to two different leak path geometries, hence leading to Model 3 (micro annulus) and 4 (channel).

3. Presentation of a base case and results

3.1. Base Case

The base case used is described in the table here below and figure 8

Well Geometry		**SI Units**		**Imperial Units**	
Well type: vertical – one casing					
Well depth (last cemented casing shoe)		1,000	m	3,281	ft
Cemented open hole		444.5	mm	17.5	in
Casing	OD	298.45	mm	13.375	in
13-3/8" – 88.2lb/ft	ID	273.31	mm	10.772	in
Gas completion (packer): None					
Material and Geology		**Young Modulus**		**Poisson's Ratio**	
Same model from surface to TD		GPa	kpsi		
Formation: Salt Rock		25	3,626	0.32	
Cement: Portland class G – 1.9sg		9	1,305	0.15	
Casing: Steel		200	29,008	0.28	
Test Conditions and Leak Path Characterization		**SI Units**		**Imperial Units**	
Test Pressure Gradient @ last cemented casing shoe		0.180	bar/m	0.80	psi/ft
Formation stresses	Vertical stresses (overburden)	0.226	bar/m	1.00	psi/ft
	Normal stresses (85% of overburden) *	0.192	bar/m	0.85	psi/ft
Downhole Temperature		38.7	°C	101.7	°F
Surface Temperature		15	°C	59	°F
Micro annulus aperture for models 1 and 3		50	µm	1.97	mil
Area of the leak path cross section for models 1, 3 and 4.		$5.33E^{-5}$	m^2	0.082615	in^2
Annular space roughness for model 4		25	µm	0.984	mil
Testing Fluid: Nitrogen (N_2), Methane (CH_4), Hydrogen (H_2). Density and viscosity are taken from REFPROP					
*For ideal creeping formations, normal stresses = 100% of vertical stresses: this case is favorable for the non-propagation of leak paths through micro annuli, as the formation will tend to "close" on the cement and the micro annulus. ** The diameter of the small channel (model 4) is constructed by keeping the same cross section area than other models 1 and 3 (full debonding cement – casing). In case of model 2, the aperture varies over depth as presented in Figure 11.					

Table 1: Presentation of the base case's parameters

For the sake of simplicity, the geometry of the leak path has also been simplified, considering a fully debonded annular space of a few dozens of micrometers (consistent with typical estimations of such leak paths diameters encountered in oil & gas wells) between the production casing and its cement sheath. This applies to the two models that require it (Darcy's and micro annulus - pipe flow driven). In addition, the case, of a small channel (tube) has also been modeled for the case of pipe flow (see figure 8 c).

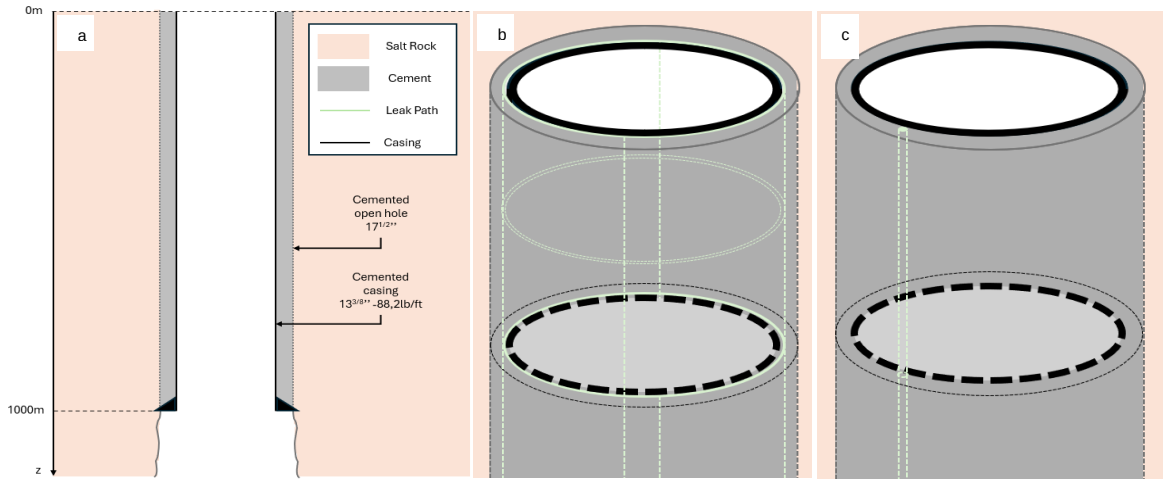

Figure 8: Illustration of the base case for the modeling of the leak through the cement sheath. (a) the well profile (b) the modeling corresponding to a complete debonding of the cement with the casing (generic case considered for the models 1, 2 and 3) (c) the case of a channel on the whole length of the well corresponding only to model 4

For all the considered models, the two additional assumptions have also been taken:

- the hypothesis of a single-phase flow of the test fluid through the micro annulus was used, and the fact that the micro annulus is probably initially filled with water was neglected: this condition would provide an additional capillary barrier prior to gas or oil flowing through the leak path.
- The flow rate is assumed to be low enough for the gas to be in thermal equilibrium with the surrounding rocks temperature (isothermal conditions).

3.2. Results

The three models described in section 2 have been applied to the base case presented in the previous paragraph 3.1.

The results are presented in the table 2 and figures 9 to 13.

		Nitrogen			Methane			Hydrogen		
		Mass leak rate	Volumetric leak rate		Mass leak rate	Volumetric leak rate		Mass leak rate	Volumetric leak rate	
		(kg/d)	(m^3/d)	(bbl/yr)	(kg/d)	(m^3/d)	(bbl/yr)	(kg/d)	(m^3/d)	(bbl/yr)
Model 1- Darcy flow in a fixed open micro annulus	Leak Rate	77.0	0.41	942	76.1	0.58	1,332	13.0	1.02	2,343
	Ratio / N_2	1	1	1	0.99	1.41	1.41	0.17	2.49	2.49
Model 2 – Darcy flow in an elastic Micro annulus	Leak Rate	76.4	0.41	942	74.0	0.58	1,332	14.2	1.12	2,573
	Ratio / N_2	1	1	1	0.97	1.41	1.41	0.19	2.73	2.73
Model 3 – Pipe flow in a fixed open micro annulus (Annular Space)	Leak Rate	114	0.6	1,378	112	0.8	1,838	19	1.5	3,446
	Ratio / N_2	1	1	1	0.99	1.3	1.3	0.17	2.5	2.5
Model 4 – Pipe flow in a vertical channel (Circ. Tube)	Leak Rate	4597	24.7	56,745	3854	29.2	67,083	1257	98.8	226,978
	Ratio / N_2	1	1	1	0.84	1.18	1.18	0.27	4.0	4.0

Table 2: Results of the simulations for the four models considered. Volumetric leak rates are given at the casing shoe conditions.

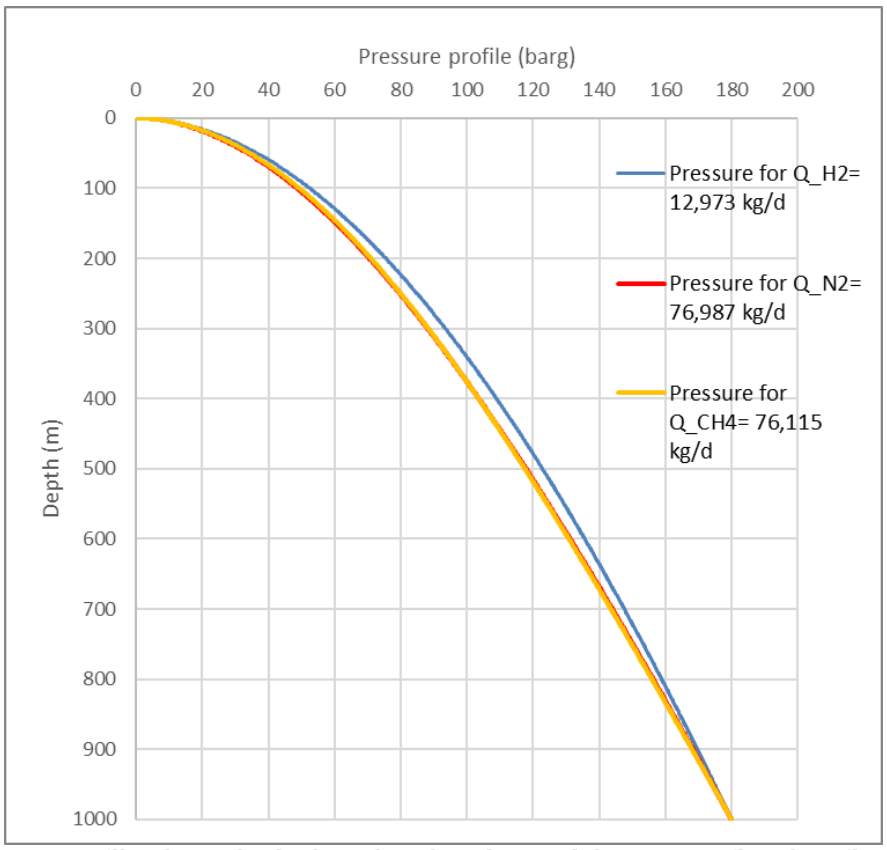

Figure 9: Pressure profile along the leak path using the Model 1 - Darcy flow in a fixed open micro annulus

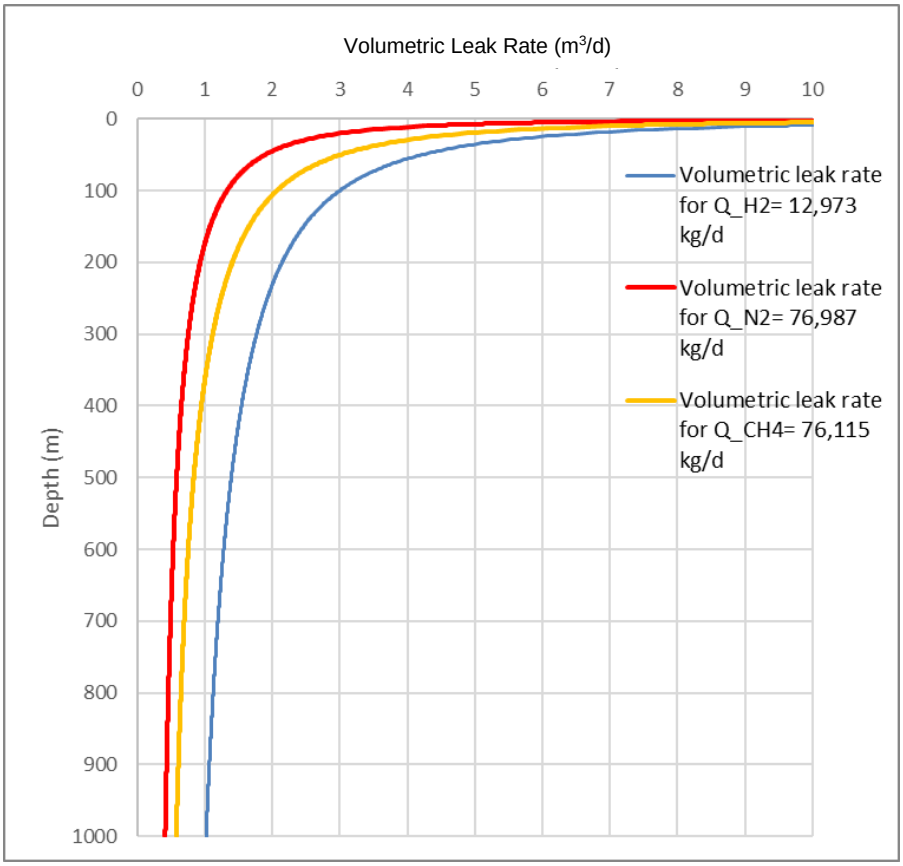

Figure 10: Flow rate profile through the leak path using the Model 1 - Darcy flow in a fixed open micro annulus

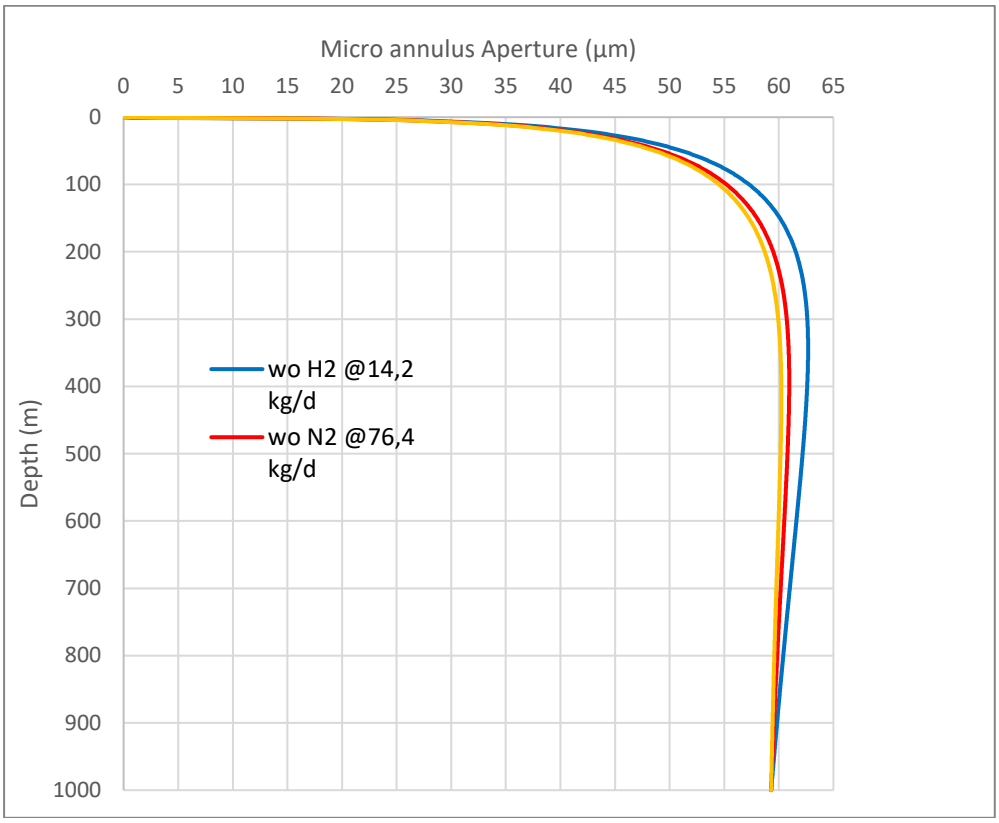

Figure 11: Micro annulus aperture along the the leak path using the Model 2- Darcy flow in an elastic Micro annulus

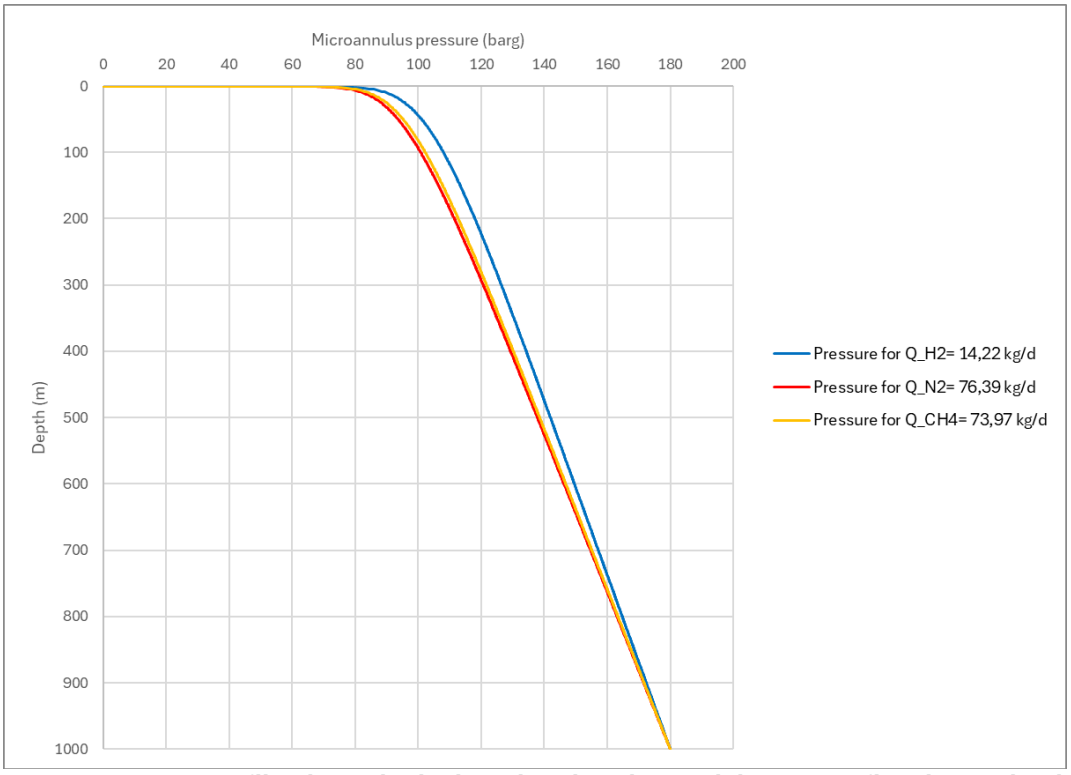

Figure 12: Pressure profile along the leak path using the Model 2- Darcy flow in an elastic Micro annulus

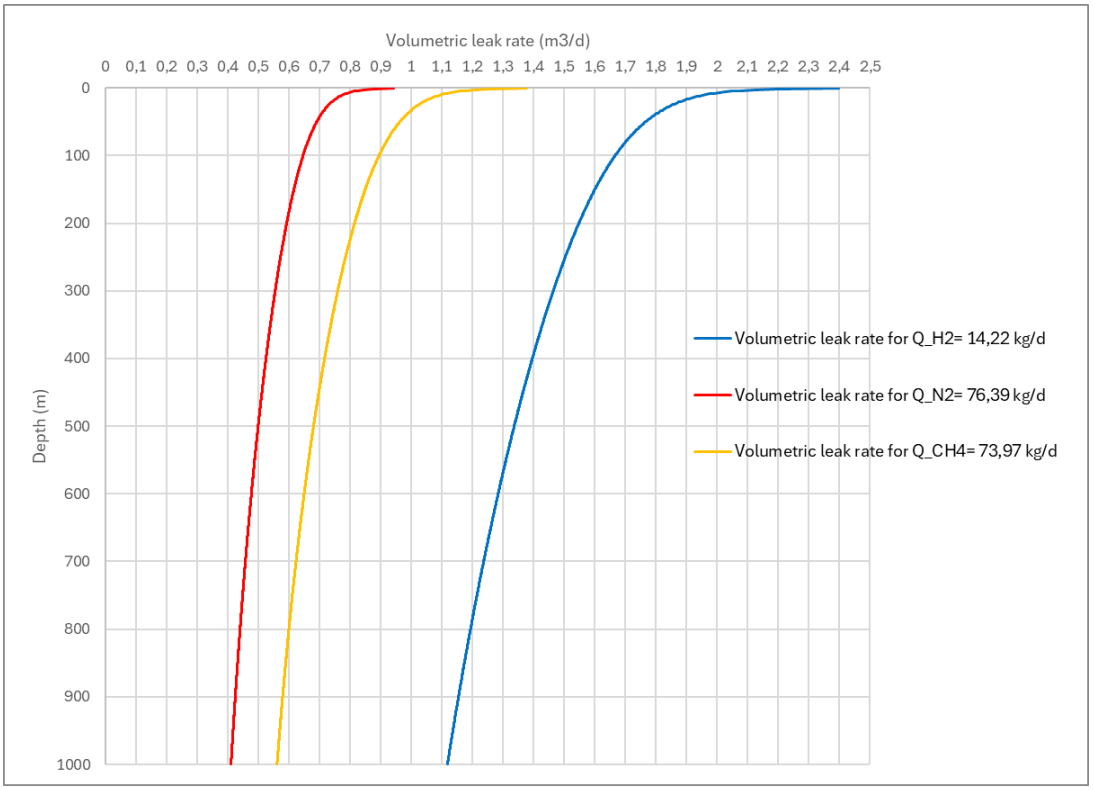

Figure 13: Flow rate through the leak path using the Model 2- Darcy flow in an elastic Micro annulus

3.3. Analysis

- The results obtained for the models 1, 2 and 3 (same base case) are quite similar: they tend to present the same order of magnitude of leak rates (slightly higher for model 3)
- In terms of leak rates ratios (Methane or Hydrogen flow compared to the Nitrogen one), the models 1,2,3 present great similarities: the mass (resp. volume) ratios found are close to 1 (resp. 1.4) for Methane and close to 0.2 (resp. 2.6) for H_2
- The comparison of results for models 3 and 4 show very different values, despite the numerous similarities of the two case studies: even though the cross sections of the leak paths are identical for both models (see table 2), the surface of contact of the fluid with the walls of the leak path are totally different which has a direct and major impact on friction forces, pressure profile and therefore leak rates. This example stresses out the importance of the models and the necessity to accurately characterize the leak path as a prerequisite.
- In terms of ratios, one can see that those ones are slightly different for model 4 than for other models: this can be explained by the fact that calculated leak rates for this 4th model are much higher than the other calculated leak rates, and therefore the ratios found between the different gases are not exactly the same for such a different range of leak rates. Performing more simulations for different case studies would enable to confirm that point.

4. Conclusions, limitations and axes of improvement

4.1. Conclusions

As a conclusion, the different modeling efforts applied to a same case study show that the ratios of leak rate between Methane, Hydrogen and Nitrogen are quite similar. This finding can be used as a mean of estimation of the leak rate for different gases.
Assuming a Nitrogen test has been performed and found as a result, interpreted in terms of mass leak rate :

$$Apparent\ Leak\ = CLR\ \pm MDLR$$

Should one want to estimate the mass leak rate that would happen with Methane or Hydrogen, using an analogy with the cases described in this paper, the following ratios Table 3 could be applied as follows:

$$Apparent\ Leak\ = CLR * ratio\ \pm MDLR * ratio$$

Ratios/ N_2	Mass leak rate	Volumetric leak rate
CH_4	1	1.4
H_2	0.2	2.6

Table 3: Proposed conversion ratios for Methane and Hydrogen compared to Nitrogen

Those ratios are taken as the mean value of results found for models 1,2 and 3. The ratios issued from model 4 have been discarded as the resulting flow rate for such a case is about 2 orders of magnitude higher than the typically accepted values for MITs accuracy and/or acceptance thresholds. Such a rate would be a significant issue and is not representative of the leak rate that are looked for during MITs.

This article also provides a methodology for a given well configuration to characterize the flow of gas through a given leak path, and provide estimates of the corresponding leak rate. On the contrary, it can also be used to estimate the size of the default / leak path if knowing the leak rate.

4.2. Limitations, Axes of improvement and further steps for the modelling

This section provides the limitations of the presented models and axes of improvement to complete the work presented in this paper.

- The validation of the different models presented is required with comparison and scaling to real case observations: in the case of a characterized leak path, it would be possible to calibrate the model and match with a given leak flow rate. With modification of the present models, the validation could also be made against pressure build up data and known leak path characterization (as proposed for example in Hatambeigi and Lackey, 2024). A real case of MIT failure, completed with a quantitative analysis of the leak path could be ideal to do such a validation and calibration work.
- The ratios proposed for this base case should be confirmed by more results obtained by performing the same approach on other cases (different pressures, size of wells, depths, temperatures, leak paths geometries).
- One could question the reliability of the models that are all using the hypothesis of single-phase flow: the leak path is likely to be initially filled with brine or drilling mud, and therefore the possibility to consider the flow and exchanges between those two fluids can impact the results. Nevertheless, it is likely that the hypotheses presented in this paper (single phase flow) represent a conservative case, as the initial presence of another fluid and capillary effects in the leak path would act as an additional barrier
- For the four models presented, the hypothesis of thermal equilibrium of the gas in the leak path with the rock mass was made, which may not be totally true, and influence the results. Nevertheless, computations using the adiabatic assumption were performed for model 3 (pipe flow) and show that the leak flow rate does not significantly change depending on the temperature assumption (adiabatic flow or in thermal equilibrium).

- The hypothesis of steady-state flow in the case of the elastic response of the micro annulus is a strong assumption that is not always applicable. A resolution of this system including a dependency over time would bring a more accurate representation of the phenomenon.
- The hypothesis of complete debonding of the cement and the casing has a major impact on the results. Looking at the resolution of such a problem for a more generic case may allow a more representative picture of a real leak path and associated flow rate.
- Similarly, the representation of a channel on model 4 by a straight vertical pipe may not be representative of the reality of such objects: a more complex geometry, introducing a more winding path, could also be encompassed as an attempt to represent more realistic leaks.

As a conclusion, particular attention should be paid when using those models in an attempt to calculate a value of flow rate for a given case. The cases presented in this work were simplified with the objective of highlighting ratios between the results obtained for different gases. The accurate characterization and representation of a specific leak path is nevertheless not straightforward and may require more detailed modelling and correct tuning of the parameters used.

5. Acknowledgements

This work is part of the FrHyGe project, supported by the Clean Hydrogen Partnership and its members Hydrogen Europe and Hydrogen Europe Research through Grant Agreement n° 101137892 — FrHyGe —HORIZON-JTI-CLEANH2-2023-1 Co-funded by the European Union. Views and opinions expressed are however those of the author(s) only and do not necessarily reflect those of the European Union or the Clean Hydrogen Partnership. Neither the European Union nor the granting authority can be held responsible for them.

We would also like to acknowledge interesting discussions with Matteo Loizzo who provided its expertise on micro annuli's modelling and behaviour. Last, we would like to thank Vanessa NDanga whose internship in 2024 participated to the initiation of the works on these topics.

6. References

Brouard Consulting and RESPEC, Analysis of Moss Bluff Cavern #1 Blowout Data, SMRI research report, 2013

Buzogany, R. Meinecke, I., 2023b. Experiences from the first H2-MITs in Northern Europe. Review of design, operational experience and results SMRI Spring 2023 Technical Conference

Crotogino, F., SMRI Reference for External Well Mechanical Integrity Testing / Performance, Data Evaluation and Assessment, 1995

Djizanne H., Stabilité mécanique d'une cavité saline soumise à des variations rapides de pression", PhD thesis, 2014

Hatambeigi, M., Lackey, G., Diagnosis of Leakage from Underground Storage Wells. Proceedings of the 2024 SMRI Spring Conference, Edmonton, Canada.

Lecampion, B.Bunger, A., Kear, J., Quesada, D., Interface debonding driven by fluid injection in a cased and cemented wellbore: Modeling and experiments, 2013

Refprop 10, National institute of standards and technology

Réveillère, The development of the concern for tightness in the salt cavern industries, of accurate tightness test techniques and of the concept of Mechanical Integrity Test, PhD Thesis, 2021

Stormont, J.C., Garcia Fernandez, S., Taha, M.R., Matteo, E.N., 2018. Gas flow through cement-casing microannuli under varying stress conditions. Geomechanics for Energy and the Environment. Vol. 13, March 2018, 1-13

Van Fossan, N. The Characterization of Mechanical Integrity for Cased Boreholes Entering Solution Caverns, 1983